# SOURCE PARAMETER ESTIMATION : EXPERIMENTAL COMPARISON BETWEEN LFM AND MLS WAVEFORMS

Gaultier Real[1], Kay L.Gemba[2], Thomas Kacel[3], and Kathrine Lamy[3]

[1]DGA Naval Systems, Avenue de la Tour Royale, BP 40915, 83050 Toulon Cedex, France
[2]Department of Physics, Naval Postgraduate School, Monterey, CA 93943, USA
[3]French Naval Academy, Lanvéoc, France

Gaultier Real, DGA Naval Systems, Avenue de la Tour Royale, BP 40915, 83050 Toulon Cedex, France. gaultier.real@intradef.gouv.fr

***Abstract:*** *For underwater source localization, accurate estimation of the time of flight (or travel time) is required and, in the case of a moving platform or a moving source, the observed waveform may include Doppler (waveform dilation). The source waveform thus needs to be sensitive to estimate both time of flight and Doppler. In this study, we compare two waveforms : Linear Frequency Modulated sweeps (LFMs) and Maximum Length Sequences (MLSs). MLSs are based on Pseudo Random Noise (PRN) signals. The performance of time of flight and relative speed estimation between the two waveforms was compared using data gathered during an at-sea experiment conducted in March 2022 near in the Mediterranean Sea, near the coast of Toulon. The trial consisted transmitting the two waveforms using a mobile source. The two waveforms presented identical center frequency (6 kHz) and bandwidth (2kHz). On the receiving end, the signals were recorded by a 192-hydrophone moored billboard array. The hydrophones were arranged in a logarithmic-spiral form to limit the influence of grating lobes in a wide frequency band. The source-array distance ranged from 2.5 to 8 km, and the source was towed at a constant speed ( 1.5m/s) and depth ( 50m). The sound speed profile was upward refracting, typical of winter Mediterranean environments. On the other hand, the bathymetry was strongly range-dependent. The analysis of the recorded signals shows that the MLS waveform outperforms the LFM waveform for estimating time of flight (uncertainty reduced by a factor 4) and radial velocity (uncertainty reduced by a factor 20).*

***Keywords:*** *Underwater acoustics, Source localization, Doppler estimation, Waveform*

# 1. INTRODUCTION

This paper focuses on the estimation of source parameters considered critical for source, or target localization [Helstrom, 2013, Van Trees Jr et al., 1968]. Typically, the estimation of Doppler and travel time is aimed [Yang et al., 2016]. The signal from a moving underwater source or target induces Doppler shift (in the narrowband case) or dilation (in the broadband case).
The use of LFM sweep provides an estimate of the travel time $\tau$ that depends on the estimated radial speed $v_r$. On the other hand, MLS, or Maximum period linear binary pseudorandom sequences, provide an unbiased and simultaneous estimate of both travel time and waveform dilation thanks to the shape of the associated ambiguity surface [Stewart and Westerfield, 1959, Duda, 1993, Pinson and Holland, 2016].
These characteristics were validated during an at-sea experiment in the Santa Barbara channel [Gemba et al., 2021].
The goal of this paper is to evaluate and compare the two waveforms performance in a range-dependent environment.
The ALMA2022 at-sea experiment was conducted near the shore of Toulon, in March 2022. On the receiving end, a $192$-hydrophone billboard array was deployed, although this paper only focuses on single-hydrophone processing. An active acoustic source was towed by the R/V JANUS II towards the shelf break. Both LFM and MLS series were transmitted and their processing is presented here.
First, the waveform characteristics are recalled in section 2. Section 3 presents the ALMA2022 experiment. The single-hydrophone results are shown in section 4.

# 2. WAVEFORM CHARACTERISTICS

## 2.1. SIGNAL MODEL

The signal received on hydrophone $k$ is shown in [Gemba et al., 2021] and the references whithin to take the following form:

$$y_k(t) = \sum_{i=1}^{I} g_i p\left(\alpha_i\left(t-\tau_i\right)\right) + n(t), \tag{1}$$

Where $p(t)$ is the transmitted waveform, $g_i$, $\tau_i$ and $\alpha_i$ are respectively the amplitude, delay and Doppler dilatation factor associated with eigenpath $i$. I is the total number of eigenpaths and $n(t)$ is some additive noise.

Two waveforms are presented and studied in this paper. First, the LFM upsweep complex envelop defined as follows [DiFranco and Rubin, 1968]:

$$\hat{p}_{LFM}(t) = e^{j\pi b(t-T_p/2)^2} \tag{2}$$

Where $b$ is the sweep rate (Hz/s) and $T_p$ is the period duration. The transmitted waveform, at carrier frequency $f_c$ is defined as:

$$p_{LFM}(t) = A\Re\{\hat{p}_{LFM}(t)\, e^{j2\pi f_c t}\} = A\cos\left(2\pi f_c t + \pi b\left(t-T_p/2\right)^2\right) \tag{3}$$

Second, the MLS [Stewart et al., 1965, Gemba et al., 2021] complex envelop is defined as:

$$\hat{p}_{MLS}\left(t\right) = e^{jm(t)\phi_L}, \tag{4}$$

where $L = 2^n - 1$ is the PRN sequence length, $m(t)$ is the continuous signal representative of the pseudorandom MLS (fully described in [Gemba et al., 2021]) and $\phi_L = \tan^{-1}\left(\sqrt{L}\right)$ is the period-matched angle. Similarly, the transmitted waveform at carrier frequency $f_c$ is:

$$p_{MLS}\left(t\right) = A\Re\{\hat{p}_{MLS}\left(t\right)e^{j2\pi f_c t}\} = A\cos\left(2\pi f_c t + m\left(t\right)\phi_L\right) \tag{5}$$

## 2.2. AMBIGUITY SURFACE

In this section, we explore the characteristics of two waveforms ambiguity functions, defined in its general form by [Woodward, 2014] :

$$\left|\chi\left(\tau, v_r\right)\right|^2 = \left|\int_0^{T_p} \hat{p}(t)\hat{p}^{\dagger}\left(\alpha(t-\tau)\right)\right|^2 \tag{6}$$

Figure 1 displays the ambiguity function $\left|\chi\left(\tau, v_r\right)\right|^2$ computed for both waveforms. A clear coupling between the estimation of $\tau$ and $v_r$ is exhibited by the LFM ambiguity surface, where local maxima are distributed along the main axis of an ellipse. The MLS ambiguity surface presents a concentration of the energy around the main lobe and offers the possibility to estimate both delays and radial velocity with better resolution.

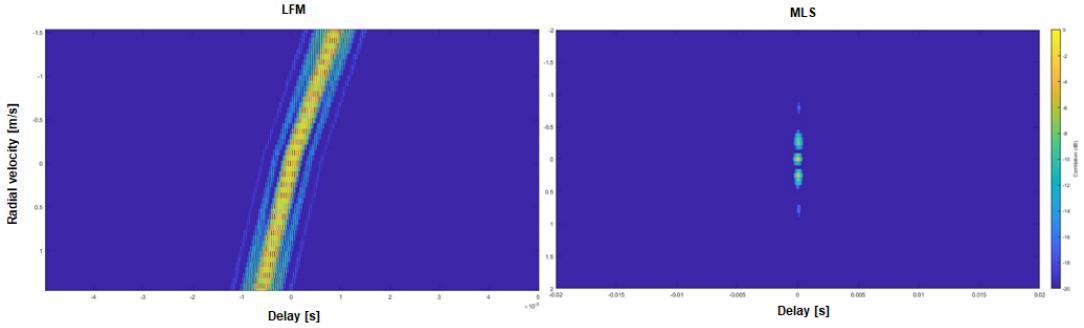


*Figure 1: (left) Ambiguity surface $\left|\chi\left(\tau, v_r\right)\right|^2$ for the LFM (left) and the MLS (right) waveforms.*

## 3. APPLICATION TO THE ALMA2022 CAMPAIGN

### 3.1. EXPERIMENTAL CONFIGURATION

The ALMA2022 [Real and Fattaccioli, 2018] at-sea campaign was carried out near the shore of Toulon, in the Mediterranean Sea, in March 2022. A 192-hydrophone passive acoustic array was deployed close to the shelf break, at a depth of 60m. The water depth at the array deployment area was 115m. Two active acoustic sources were installed in a tow-fish and towed away

from the array while transmitted various sequences of signals. The source depth was 50m and the towing speed was maintained as constant as possible 1.5m/s. The maximum range was 8km, allowing the tow-fish to navigate in water as deep as 1300m.
The sound speed profile was slightly upward refracting, as typical of the area and season. The deployment area, the passive acoustic array and the transmitted sequences are depicted, alongside with a BELLHOP ray trace, in Figure 2.
Series of MLS and LFM at center frequency $f_c = 6$kHz were transmitted every 150s.

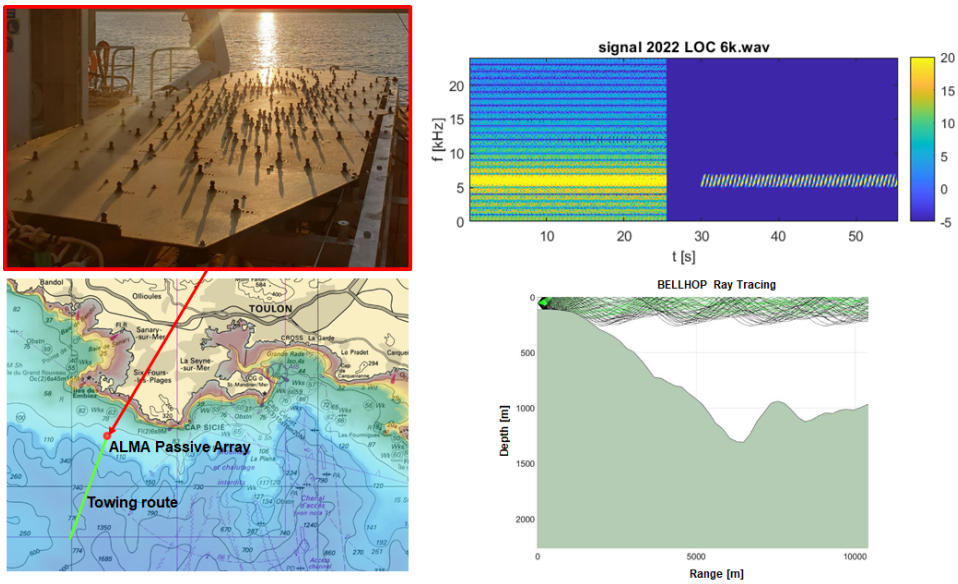


*Figure 2: (top-left) ALMA 2022 passive acoustic array on the deck of the R/V JANUS. (top-right) Transmitted waveforms: MLS ( 0 to 25s) and LFM (30 to 55s). (bottom-left) ALMA 2022 area and bathymetry. (bottom-right) Ray trace for the source at 50m depth at maximum range.*

## 3.2. RECEIVED SIGNALS AND PERFORMANCE

The MLS and LFM sequences were received and analyzed on a single hydrophone close to the acoustic center of the array. Signal to noise ratio (SNR) was sufficient to conduct the analysis on a single sensor. Nonetheless, combining this study with array processing capabilities is of interest.
The received signals were bandpass filtered and the experimental ambiguity surface was computed according to:

$$|\hat{\chi_k}(\tau, v_r)|^2 = \left| \int_0^{T_p} y_k(t) \hat{p}^\dagger (\alpha(t-\tau)) \right|^2 \tag{7}$$

They are displayed in Figure 3. Extracting the maxima of the ambiguity surface leads to an estimation of both delays and Doppler dilatation factor for each eigenray.

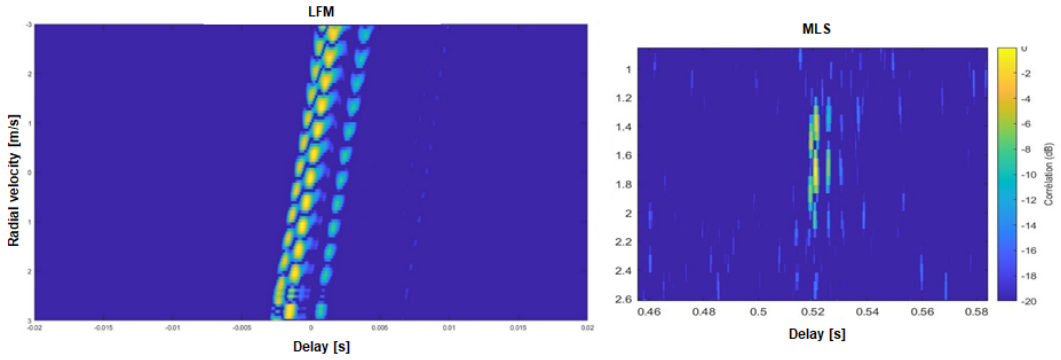


*Figure 3: (left) Ambiguity surface $|\hat{\chi}_k(\tau, v_r)|^2$ for the LFM (left) and the MLS (right) received signals.*

Our study focuses on the most energetic eigenray. Hence, only one local maximum is extracted for every received signal. This corresponds to a maximum search on ambiguity surfaces such as that of Figure 3. We can then track the evolution of the estimated time delay and radial velocity for each detected LFM/MLS. $50$ consecutive estimates are therefore available for one received sequence.
For a typical received LFM series, the estimation of the radial speed is greatly fluctuating, oscillating around the ground truth with considerable variations (roughly 1m/s). On the contrary, the radial speed estimated over a series of MLS is extremly consistent. Figure 4 displays this result for a series of $50$ received waveforms.

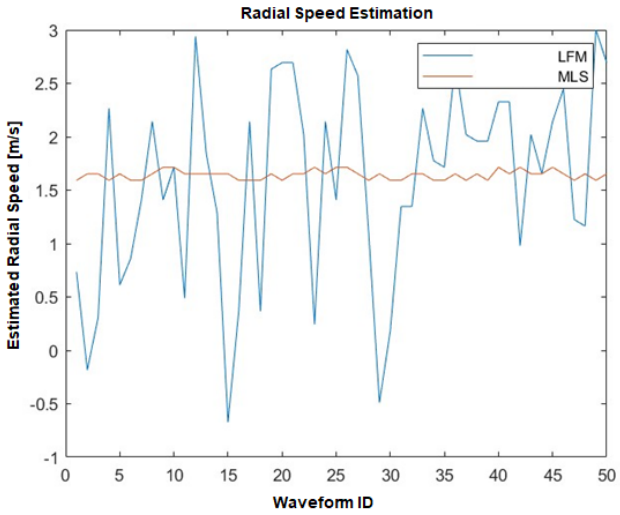


*Figure 4: Estimated $v_r$ from a series of LFM (blue) and a series of MLS (ref). Ground truth is $1.5$m/s.*

Similarly, the time of arrival of the most energetic eigenpath can be estimated. The change in travel time was detrended from the support vessel motion using a second-order polynomial regression. The results are presented in Figure 5 and confirm that MLS waveforms outperform LFM waveforms, this time by a factor $4$ on estimated travel time uncertainty $\Delta\tau$. This estimation was performed on $25$ series of $50$ waveforms.

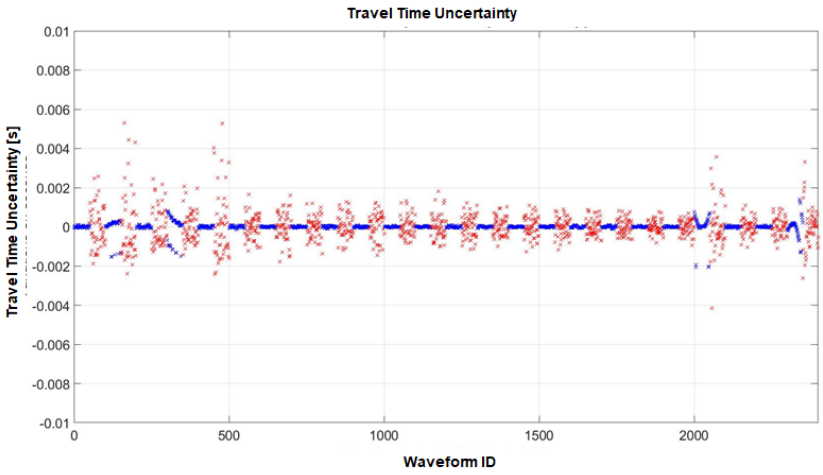


*Figure 5: Estimated $\Delta\tau$ from 25 series of LFM (red) and a series of MLS (blue).*

## 4. CONCLUSION

This paper presented a study similar to that conducted in [Gemba et al., 2021], comparing the capabilities of LFM and MLS waveforms to provide an accurate estimation of a moving source radial speed $v_r$ and travel time $\tau$. After recalling the theoretical characteristics of the two studied waveforms, we focused on the evaluation of the ambituity surface on at-sea data. The latter were acquired during the ALMA2022 experiment, in an environment that differs from that of the original study by its range-dependence.
The MLS waveform outperforms the LFM waveform by a factor 20 on radial speed estimation and by a factor 4 on travel time uncertainty estimation.
Although a 192-hydrophone billboard array was used at the receiving end, no array processing was performed at the time. A beamforming step prior to the match filter operation would provide spatial information about the received signals, increasing the localization capabilities.
For computing efficiency, baseband processing and frequency domain beamforming would need to be considered.

## 5. ACKNOWLEDGEMENTS

The authors thank the participants to the ALMA2022 campaign, including the companies ALSEAMAR and SAAS/COMEX.

## REFERENCES

[DiFranco and Rubin, 1968] DiFranco, J. V. and Rubin, W. L. (1968). *Radar detection*. Prentice-Hall.

[Duda, 1993] Duda, T. F. (1993). Analysis of finite-duration wide-band frequency sweep signals for ocean tomography. *IEEE journal of oceanic engineering*, 18(2):87–94.

[Gemba et al., 2021] Gemba, K. L., Vazquez, H. J., Fialkowski, J., Edelmann, G. F., Dzieciuch, M. A., and Hodgkiss, W. S. (2021). A performance comparison between m-sequences and linear frequency-modulated sweeps for the estimation of travel-time with a moving source. *The Journal of the Acoustical Society of America*, 150(4):2613–2623.

[Helstrom, 2013] Helstrom, C. W. (2013). *Statistical theory of signal detection: international series of monographs in electronics and instrumentation*, volume 9. Elsevier.

[Pinson and Holland, 2016] Pinson, S. and Holland, C. W. (2016). Relative velocity measurement from the spectral phase of a match-filtered linear frequency modulated pulse. *The Journal of the Acoustical Society of America*, 140(2):EL191–EL196.

[Real and Fattaccioli, 2018] Real, G. and Fattaccioli, D. (2018). Acoustic laboratory for marine applications: Overview of the alma system and data analysis. *OCEANS 2018 MTS/IEEE Charleston*, pages 1–7.

[Stewart et al., 1965] Stewart, J. L., Allen, W., Zarnowitz, R., and Brandon, M. (1965). Pseudorandom signal-correlation methods of underwater acoustic research i: Principles. *The Journal of the Acoustical Society of America*, 37(6):1079–1090.

[Stewart and Westerfield, 1959] Stewart, J. L. and Westerfield, E. (1959). A theory of active sonar detection. *Proceedings of the IRE*, 47(5):872–881.

[Van Trees Jr et al., 1968] Van Trees Jr, H. L., Baggeroer, A. B., Collins, L., Kurth, R., and Cruise, T. (1968). Detection and estimation theory. Technical report, Research Laboratory of Electronics (RLE) at the Massachusetts Institute of ….

[Woodward, 2014] Woodward, P. M. (2014). *Probability and information theory, with applications to radar: international series of monographs on electronics and instrumentation*, volume 3. Elsevier.

[Yang et al., 2016] Yang, L., Yang, L., and Ho, K. (2016). Moving target localization in multistatic sonar by differential delays and doppler shifts. *IEEE Signal Processing Letters*, 23(9):1160–1164.